Reconstruction of Clean and Adsorbate-Covered Metal Surfaces

S. Titmuss, A. Wander, and D. A. King*

Department of Chemistry, University of Cambridge, Lensfield Road, Cambridge CB2 1EW, UK

Received October 5, 1995 (Revised Manuscript Received April 3, 1996)

Contents

I. Introduction

The study of surfaces and surface processes has developed greatly over the last 30 years.[1,2] New techniques are continually being developed to study ever more complex aspects of clean surface properties and of surfaces with adsorbates. The most fundamental piece of information available from a surface science investigation is the location of atoms at the interface: surface crystallography.

A surface represents a highly asymmetric environment, with both the coordination and the electronic structure of the surface atoms being modified from their bulk values. As a result, the structure of the surface may be very different from a simple bulk termination model. This modification may take the form of relaxations and displacements, where interlayer and intralayer spacings are altered, or more dramatic modifications involving large-scale mass transport of atoms across the surface leading to radical changes in coordination of surface atoms, and in the surface layer symmetry.

Although such effects have been identified for clean metal surfaces[3] it has been traditional for the surface layer to be modeled as a rigid, bulk-terminated layer in studies of adsorption; the so called "checker board" model. Primarily this assumption was made because the available methods of structure determination, and in particular the state of LEED,[4] were incapable of handling the greater complexity inherent in the problem once surface layers are allowed to reconstruct. An *a posteriori* rationale for this approach is that it is often the case that the adsorbate layer in some way returns the surface layer to its ideal bulk-terminated coordination.

This picture has now changed. In particular, new techniques[1,2,5,6] are available which allow the full determination of the geometry of not just the adsorbed layer, but also of the surface atoms in the interface region. On the basis of the results of clean surface studies, the top few layers of the metal (the interface region) are generally found to be involved in a reconstruction. This work has led to the rigid lattice model being replaced by a picture of a mobile, plastic surface capable of responding to the presence of adsorbate atoms or molecules through structural modifications.

We begin our review by looking at clean metal surfaces and identifying the simplest class of reconstruction, relaxation of the top few metal layers. With a few exceptions, this type of behavior can be understood in terms of a local valence electron density model. We will then turn to more complex classes of reconstruction involving mass transport, and hence changes in packing density, within the surface layers comprising the clean metal surface. Again, such effects can be understood within the framework of relatively simple local electron density models.

Studies of adsorbate atoms and molecules are less advanced than clean surface studies since the increase in complexity leads to a great increase in the number of parameters which need optimizing in a structural study. However, significant progress has been made, and we will review a few of the results, ideas and trends seen in the literature.

Finally, we will turn to consider the next generation of surface crystallographic studies by identifying some of the problems which still exist, and some of the great challenges remaining within this active and lively field. In a short review of this length, we cannot hope to comprehensively review all surface structures determined to date. Such a list is already available elsewhere.[7] Instead, we have selected representative examples of interesting and challenging structural determinations to illustrate the ideas being discussed.

II. Relaxation and Reconstruction of Clean Metal Surfaces

In this section we review the results of structural studies of clean reconstructed metal surfaces. Reconstructions can be divided into a number of classes.

S0009-2665(95)00214-7 CCC: $25.00

Simon Titmuss received a B.A.(Hons.) in Natural Sciences from the University of Cambridge in 1994 and is currently working toward a Ph.D. with Professor King in the Department of Chemistry at the University of Cambridge.

Adrian Wander is a University Assistant Lecturer in the Department of Chemistry at the University of Cambridge. His research covers fundamental aspects of surface structure.

David King is the 1920 Professor of Physical Chemistry in the Department of Chemistry at the University of Cambridge, and is currently Head of Department. In 1995 he was elected Master of Downing College, Cambridge. His research covers structure and dynamics at surfaces and heterogeneous catalysis.

The majority of materials undergo a simple relaxation in which only the interlayer spacings change (section II.A). However, a number of surfaces undergo more dramatic changes. These may involve lateral displacements of atoms, within the surface layers (section II.B), or a change in the surface layer atomic density (section II.C). The most widely known reconstruction is probably the fcc {110} missing row reconstruction (section II.D) which displays all of these effects within the top three surface layers.

A. Relaxations

The relaxation of the outermost layer of a metal surface away from its ideal bulk-terminated position was first identified by low-energy electron diffraction[8] in studies of the relatively open {110} surfaces of fcc metals (Al{110}[9,10] and Cu{110}[11]). This was found to be a contraction of ~10% for both surfaces, and such contractions are now recognized as a near universal property of virtually all metal surfaces. Subsequent reanalysis of the above structures[3,12−14] by LEED has shown that relaxation effects can extend several layers into the material. The results of the reanalysis of Al{110} by Andersen et al.[14] are shown in Figure 1. The relaxation appears to be oscillatory in nature, with the oscillations decaying rapidly into the bulk. These studies have been concentrated on the relatively open, low coordination number {110} surfaces of fcc metals. However, recent advances in surface crystallographic techniques[5] mean that the much smaller relaxations of close-packed surfaces can now be resolved (e.g Rh{111},[15] Figure 2).

At the heart of these effects is the redistribution of electron density, which occurs at the surface, and can be thought of as due to a desire of the atoms to reside in an area of optimum local electronic density. Finnis and Heine[16] first suggested that the electron density of the surface would relax to produce a

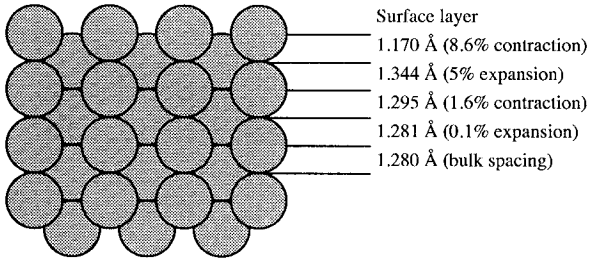

Figure 1. Cross sectional view through the Al{110}[14] surface showing the damped oscillatory nature of the changes in interlayer spacing.

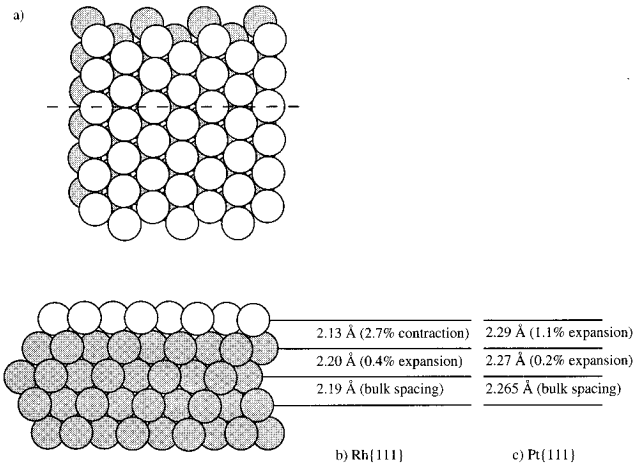

Figure 2. (a) Plan view of the fcc {111} surface. Cross sectional views through (b) the Rh{111} and (c) the Pt{111} surfaces showing the damped oscillatory nature of the changes in interlayer spacing and the anomalous expansion of the first interlayer spacing of Pt{111}.

smoother distribution, as if it possessed surface tension. This redistribution of electron density gives rise to a net inward force on the surface atoms causing the observed contraction of the first to second interlayer distance. Subsequently, Landman et al. showed that the redistribution of electronic density will extend over several layers, giving rise to the observed damped oscillatory nature of the relaxation.[17]

These results can be visualized within the framework of effective medium theory.[18] The coordination, and consequently the electron density, around the surface atoms is reduced by the loss of neighboring atoms necessary to create the surface. Consequently, the surface layer atoms are relaxed inward, to increase their local embedding charge density. Without further relaxation this would leave second layer atoms in a relatively high region of local electron density, and consequently the second to third layer spacing is increased compared to the bulk spacing, lowering the local electron density to the optimum value and giving rise to an expansion. This same argument can then be extended into the bulk, giving rise, together with electron shielding, to the observed damped oscillatory nature of the relaxations.

However, there are a number of apparently anomalous results which indicate an expansion of the first to second layer distance relative to the bulk interlayer spacing. Such effects have been reported by LEED for Pt{111},[19] Pd{100},[20] Rh{100},[21] and Pd{111}.[22] Two of these studies (Pd and Rh) are characterized by relatively poor agreement between theory and experiment, but in the study of Pt{111} there is excellent agreement, suggesting that the expansion is a real effect (Figure 2). In order to provide a possible explanation for these effects it is necessary to extend the simple picture presented above by including the effects of the d electrons.

The bulk lattice constant of transition metals is a balance between the outward pressure, exerted by the delocalized sp electrons, and an inward force due to the localized d electrons.[23] In the simple case of contraction, the sp electrons spill over into the vacuum producing a net inward force due to the d electrons. Methfessel et al.[24] used this model to examine the contraction of the 4d metal surfaces. The contraction is found to be a minimum (close to 0%) for Pd due to the nearly complete occupancy of the metal d band. However, experiment shows an expansion of 3%, which must therefore be due to some other physical effect. Quinn et al.[20] suggest the possibility of magnetic moment effects or even the possibility of interstitial hydrogen expanding the lattice. For Pt{111}, Materer et al.[19] suggest that the expansion is due to a weakening of the interlayer bonding in favor of intralayer bonding. Such an argument is consistent with the high value of surface stress calculated for Pt{111},[25] and with the fact that at high temperature Pt{111} reconstructs through an isotropic compression of the surface layer.[26] At room temperature Au{111} shows a similar increase in the atomic density of the surface layer,[27] accompanied by an expansion of the first interlayer spacing. The measured expansion for Pt{111} of $1.3 \pm 0.4\%$[19] is in close agreement with the 1.25% expansion calculated by Feibelman et al.[28] using first principles local density functional theory. A full explanation of the few observed expansions must await further total energy calculations.

B. Displacive Reconstructions at Constant Layer Density

In addition to relaxation of the interlayer spacings some surfaces undergo displacive intralayer lateral relaxations within surface layers, lowering the layer symmetry but not the density.

Within this class of displacive reconstructions the low temperature c(2×2) reconstruction of W{100} was the first to be discovered and is now the most extensively investigated. From an analysis of the observed space group symmetry of the LEED pattern Debe and King found that surface layer W atoms are laterally displaced to produce a zigzag atomic arrangement,[29] shown in Figure 3. Subsequently, a full LEED study supported this model and gave a lateral displacement of 0.16 Å accompanied by a contraction of the first to second layer distance by 6%.[30] On the basis of theoretical studies it was suggested that the reconstruction of W{100} was actually a multilayer process[31,32] which was subsequently experimentally confirmed.[33−35] The structure, now firmly established, involves a displacement of the topmost layer of W atoms by 0.24 Å with a displacement of the second layer atoms in the same direction by about 20% of this value.

Fu and Freeman[31] proposed that these second layer displacements are driven by a combination of symmetry lowering and elastic strain. The displacement of the first layer atoms causes them to roll on top of the second layer atoms, giving rise to a large strain which can be relieved by a small displacement of the second layer atoms. The reconstruction is driven by electronic effects in the first layer and by strain effects in the second layer. Again, we have an example of a damped reconstruction extending into

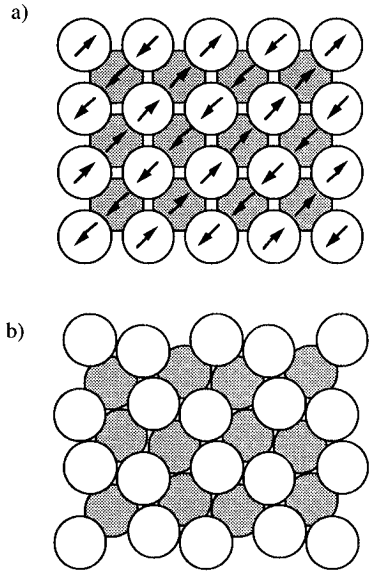

Figure 3. A plan view of the c(2×2) reconstruction of W{100}. In (a) the displacement tendencies of the atoms away from their ideal bulk terminated positions are indicated, while (b) displays the final two layer Debe−King structure resulting from these displacements.[29,34,35]

the bulk of the material, suggesting that such effects should be considered the rule for all materials. In a metal the influence of the surface is fully attenuated within about four layers.

While the structure of the multilayer reconstruction and the mechanism behind the second layer reconstruction are well understood, there is still some uncertainty over the exact nature of the electronic driving mechanism behind the reconstruction of the first metal layer.[36]

C. Changes in Surface Layer Atomic Density

Large-scale surface reconstructions producing changes in the surface layer density were first identified on Pt{100}.[37] The first layer of Pt reconstructs from the square lattice of an fcc {100} surface into a near hexagonal arrangement leading to the surface being known as the hex phase.[38] Subsequently other fcc {100} surfaces have been shown to undergo similar reconstructions (Au{100}[39,40] and Ir{100}[41]). These reconstructions are again related to optimal embedding charge density, surface stress, and the redistribution of surface electronic density.

Models have been proposed for all these surfaces on the basis of LEED patterns. The reconstruction of Au{100}, described as c(26×68), is thought to involve a buckled hexagonal Au layer sitting on top of an unreconstructed substrate layer.[40] A similar model has been proposed for both the hex and hex-R reconstructions of Pt{100} (Figure 4) which differ only in a rotation of the hexagonal layer relative to the underlying substrate.[46,47] The Ir{100}-(1×5) reconstruction is similar, involving a slight distortion of the top layer away from a perfect hexagonal overlayer.[46,47]

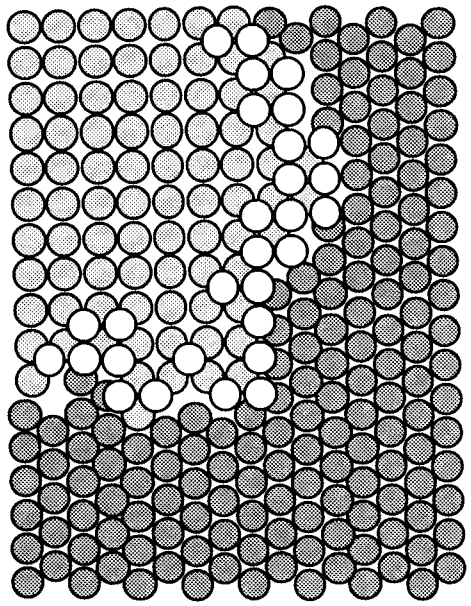

Figure 4. A plan view of the reconstruction of Pt{100}-hex to the (1×1) phase induced by CO. The adsorbate is not shown. The darker shaded atoms represent the reconstructed hex surface, the lighter shaded atoms represent the unreconstructed (1×1) surface, and the unshaded atoms a second layer of (1×1) surface, above the surface plane, generated by the reduction in surface atomic density as the (1×1) surface is generated from the hex. The dynamics of the transition from hex to (1×1) follow a strongly nonlinear power law,[42] which is an important factor in the oscillatory reactions of CO on Pt{100}.[43−45]

The interpretation of the LEED patterns led to models in which only one layer of the metal is reconstructed. This picture has been supported by high-energy ion scattering measurements,[48] which show that only one layer of the metal is significantly displaced from bulk positions. The reconstructions are driven by the need for surface atoms to relocate into a region of higher electron density. Whereas with some metals this is achieved by a simple contraction of the first to second interlayer distance, in this class of metals the surface stress is reduced by increasing the embedding charge density in a reconstruction with a more dense, fcc {111}-like arrangement in the top layer. The fcc {111} surface is thermodynamically the most stable, and it is also the smoothest surface. In the absence of reconstruction, surface atoms behave as if the surface experiences surface tension. Opposing this contraction and rearrangement is the resulting loss of optimal bonding between the first and second metal layers—the interlayer resistance. The mismatch between top and second layers gives rise to a buckling of the reconstructed hexagonal layer, which for Ir{100} has been measured by LEED to be 0.48 Å,[49] and for Pt{100} has been measured by He diffraction,[50] and in the STM images of Behm et al.[51] and most strikingly of Borg et al.,[52] to be 0.4−0.5 Å (Figure 5).

The buckling of these surfaces suggests that the reconstruction will actually extend several layers into the surface since the second layer atoms are in far from ideal surroundings. This will presumably involve relaxation and buckling effects, but the full determination of the reconstructed surface structures of Pt{100} and Au{100} is currently beyond investigation, by experiment or theory, due to the large size of the surface unit cell.

This simple picture of the reconstruction of some fcc {100} surfaces into close-packed, fcc {111}-like planes under the action of surface stress, overcoming the interlayer resistance, also underlies the room temperature reconstruction of the already close-packed Au{111} surface. Here the contraction and buckling of the topmost layer have been resolved by both He diffraction[53] and STM.[54] This surface undergoes a uniaxial contraction of 4%.[46,47]

As with simple relaxations, the driving force behind these effects is the redistribution of surface electronic density, which gives rise to a high surface stress in the unreconstructed surfaces. Total energy calculations[55] have shown that reconstruction is likely when the in-plane surface stress is high, and the interlayer resistance is small. High surface stress is created by a depletion of the surface d electron density causing a reduced antibonding contribution at the surface. This is particularly important for the 5d metals where relativistic effects deplete the d electron density in favor of sp occupancy. As a result of this stress, surface atoms undergo a change in intralayer bonding rather than a change in interlayer bonding. The relief of the surface stress lowers the total energy; in the case of Pt{100} recent microcalorimetric measurements[56] show that the reconstructed hex

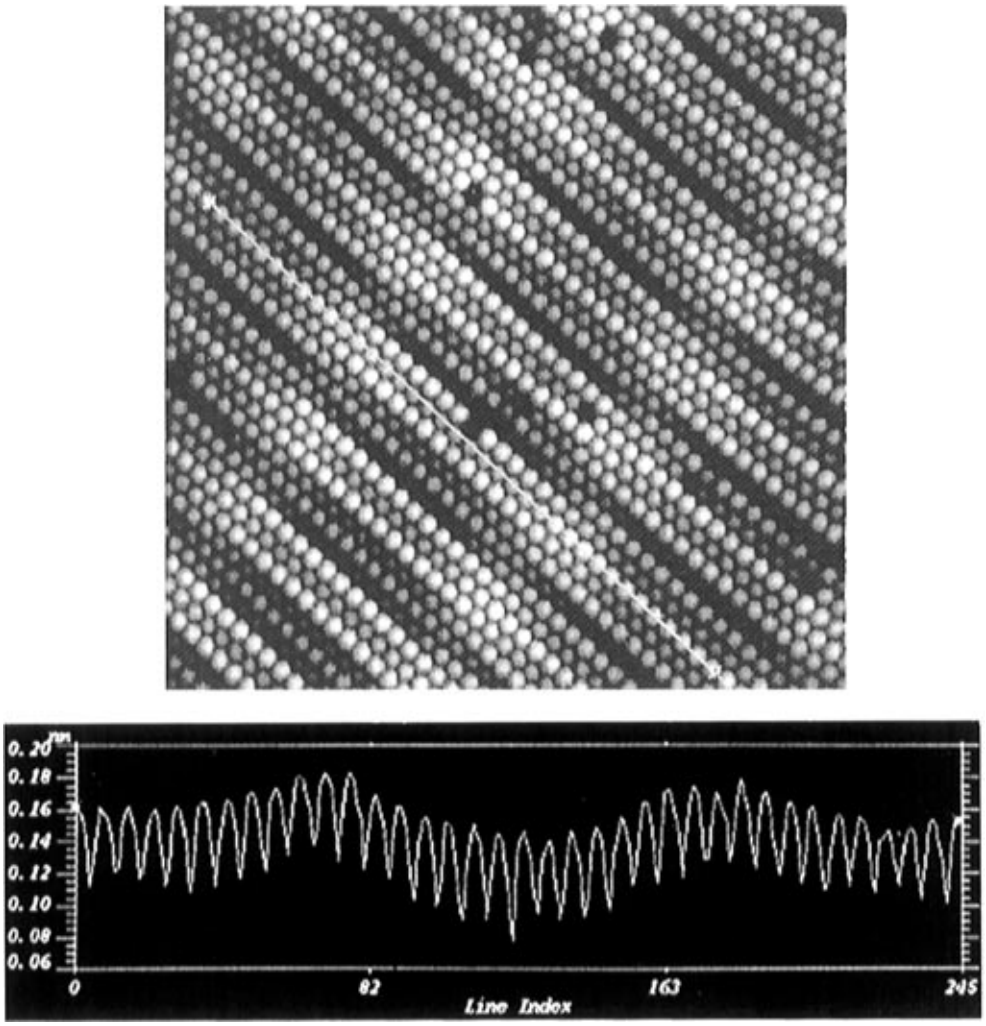

Figure 5. STM Image of the Pt{100}-hex phase, with the corrugation along [$\bar{1}$5] shown in the line profile. (Reprinted from ref 52. Copyright 1994 Elsevier.)

phase is 20 ± 3 kJ (mol Pt)$^{-1}$ lower in energy than the (1×1) surface. The change in atomic density for the reconstructed {100} surfaces of Pt, Ir, and Au is around 20%, showing that large-scale mass transport is involved. Finally, we note that these reconstructions are limited to the late 5d metals, for which surface stress is high and the interlayer resistance is low. A similar mechanism lies behind the reconstructions of the already close-packed Au{111} and Pt{111} surfaces discussed in section II.A.

D. Missing Row Reconstruction of fcc {110} Surfaces

A well-known class of reconstructions sharing some similarities with each of the above two classes is the missing row reconstruction of fcc {110} surfaces. The {110} surface is the most open of the widely studied low Miller index fcc surfaces. Consequently, it has the lowest surface layer atomic density and the highest surface energy, making it the most likely to reconstruct. In the case of Ir, Pt, and Au the clean {110} surface spontaneously reconstructs, giving rise to the (1×2) missing row reconstruction.[57−60] This model was first proposed by Chan et al.[59] to explain the (1×2) periodicity observed in the LEED pattern of clean Ir{110} and consists of a surface in which every other row in the ⟨110⟩ direction has been removed, although recent STM data has shown that the structure may be rather more complex.[61] The {110} surface of the 3d metals (Ni and Cu) and 4d metals (Ag and Pd) appear to be stable to this reconstruction, but the missing row reconstruction can be stabilized by a small quantity of alkali adsorbate.[62−64]

Again, this is a multilayer reconstruction, with pairing of atoms in both the second and fourth layers[65] and rumpling in the third (Figure 6). On Au{110} this pairing involves lateral displacements of the atoms by ∼0.05 Å in both layers. The third layer is buckled by 0.24 Å and the topmost layer is strongly relaxed, with a contraction of the first to second layer distance of 20%. These effects seem to be consistent for all missing row-type reconstructions, with Pt{110} undergoing a multilayer reconstruction of a very similar nature.[66−68] Consequently, the missing row reconstructions show all three effects discussed above: a relaxation of the first to second interlayer distance; a change in the surface layer atomic density; and a displacive reconstruction of the second and fourth layers parallel to the surface; accompanied by a buckling of the third layer.

Removal of close-packed rows of material from the {110} surface produces ribbons of {111}-like microfacets across the surface, which have been imaged

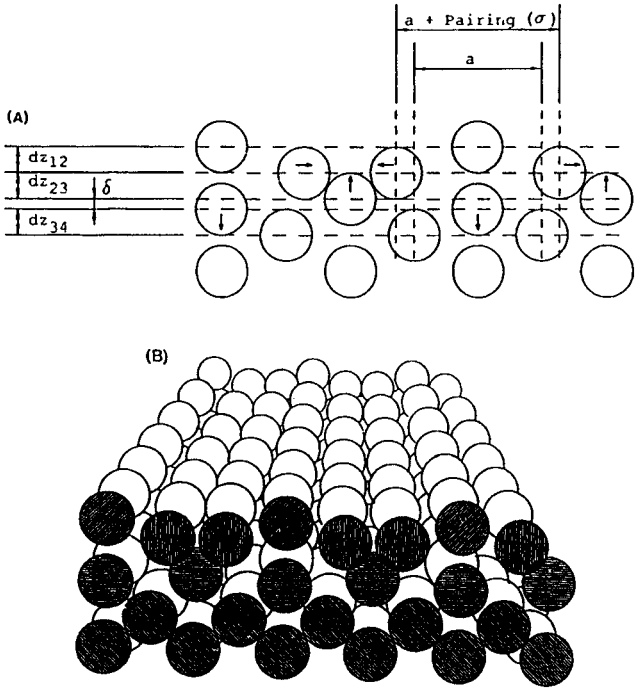

Figure 6. The missing row reconstruction on fcc {110} surfaces, showing, in (a), the second layer row pairing and third layer buckling. The top layer also relaxes downward producing a relatively smooth surface, shown in b.[78] All fcc {110} missing row reconstructions exhibit similar effects, even those induced by the presence of adsorbates on stable clean (1×1) surfaces.

directly by STM.[69,70] The creation of these {111} microfacets has often been cited as the driving force for the missing row reconstruction. The bonding in these systems is again a competition between the localized repulsive interaction of the d electrons and the bonding nature of the delocalized sp electrons. The creation of a missing row structure, with its smooth fcc {111} microfacets, allows the sp electrons to become more delocalized, lowering the electronic kinetic energy, without increasing the number of nearest neighbor broken bonds and thus leading to an increase in the bonding character of these surfaces,[71] suggesting that the missing row structure is associated with a lowering of the surface electronic density. The lower electronic density found for 4d metals provides a possible explanation of their stability toward this class of reconstruction. This may also explain the observations that alkali metals, at low coverages, induce missing row reconstructions, since the addition of an alkali metal atom to the surface leads to an increase in the s electron density at the unreconstructed surface, which is then lowered back to an optimum value by the development of the missing row reconstruction. However, this model predicts that the surface should be more stable with larger facets, suggesting that (1×*n*) reconstructions should become increasingly stable with increasing n, contrary to observation. The overriding stability of the (1×2) surface has a different origin.

Theoretical investigation of the missing row reconstruction supports the multilayer nature of the process.[71] These mutilayer relaxations provide a route to the alternative driving mechanism. Row pairing in the *second* layer creates open channels into which the remaining top layer atoms can relax, restoring their local valence electron density and producing a 20% contraction of the first interlayer spacing. The first and second layers then together create a compact, high-density surface resembling the rumpled top layer on Pt{100} hex. The missing row reconstruction is thus stabilized as it creates, through the multilayer relaxations, the most dense atomic packing possible at a {110} surface. The buckling of the third layer further lowers the surface energy. These similarities with the Pt{100} hex reconstruction suggest that the driving force for the combined row pairing and missing row reconstruction is again the high surface stress of the late 5d transition metals.

E. Summary of Clean Surfaces Effects

The above demonstrates that the concept of a rigid, bulk-terminated surface lattice is no longer tenable. The surface is a dynamic environment with atomic displacements occurring several layers into the bulk region. Most surfaces undergo a straightforward multilayer relaxation (section II.A) driven by the movement of surface atoms into new locations which restores their local optimum electron density. Displacive reconstructions, which preserve the overall atomic density of the surface layer, can also occur (section II.B). Surface stress plays a critical role in the large-scale surface reconstructions, involving layer density changes, for Pt, Au, and Ir. Here, the surface atoms are rearranged to optimize the local charge density by modifying the in-plane bonding as well as the interlayer bonding (section II.C). These effects often occur in combinations. W{100} shows displacive effects and relaxation effects, while the most dramatic example is seen in the fcc {110} missing row reconstructions (section II.D), in which all three effects occur.

The stability of the close packed fcc {111} surfaces is well demonstrated, although Au{111} does undergo a reconstruction to an even more close-packed top layer at room temperature. This stability can be seen as another unifying theme running though several surface reconstructions. The fcc {100} pseudo hexagonal reconstructions and the fcc {110} missing row reconstructions involve the surface producing more close packed surface layers, thereby reducing the deficit in electron charge density at surface atomic positions.

III. Adsorbate-Induced Reconstructions

While a great deal of work has been devoted to studies of clean surfaces and clean surface reconstructions, adsorbate-induced reconstructions have received less attention to date. The introduction of an adsorbate introduces extra degrees of freedom into the problem and hence greatly complicates the structural analysis. However, progress has been made in this field and is reviewed here.

The formation of a chemical bond between a surface layer metal atom and an adsorbed molecule will clearly alter the local embedding charge density experienced by the metal atom. It must therefore be expected that the clean metal surface structure is altered by chemisorption and will be critically de-

pendent on the nature and density of the adlayer. In general metal surface layer atoms should restructure into lower density arrangements to reduce the local charge density.

A. Atomic Adsorbates

Atomic adsorbates represent potentially the simplest form of overlayer on metal surfaces. Consequently, reconstructions induced by atomic adsorbates have received more attention than molecular adsorbates. The first observations of the restructuring of clean surfaces by atomic adsorbates, made in the late 1970s, were of displacive structural changes on W{100}, where H adatoms were found to produce a rotation of the Debe-King clean surface structure,[36] and on Ni{100}, where carbon adatoms were found to produce a clock reconstruction. These are both described in more detail in section III.A.2 below. Since that time a substantial range of adsorbate-induced reconstructions have been studied; including relaxation as a class of reconstruction, the phenomenon is universal for chemisorbed species.

1. Adsorbate-Induced Reconstructions of fcc {110} Surfaces

Although some clean fcc {110} surfaces are unstable with respect to layer density reconstructions (section II.D.), the clean {110} surfaces of Ni, Cu, Pd, and Ag are not, but they do show the large relaxations expected for atomically rough surfaces (section II.A).[11−13,72−77] However, these surfaces restructure with a wide range of atomic adsorbates,[78] demonstrating that the clean surfaces are only just stable with respect to these reconstructions.

Exposure of the clean {110} surfaces of Ag, Pd, Cu and Ni to alkali metal atoms gives rise to (1×2) structures.[62−64,79] Hayden et al.[62] suggested that this was the result of a reconstruction rather than due to the formation of an ordered overlayer and further suggested that the adsorbate-induced structure, on Ag{110}, was the missing row model (section II.D). The alkali adsorbate occupies the channels created by the removal of close-packed rows from the surface. Similar effects have been observed for Cs adsorbed on Pd{110},[63] and detailed LEED studies[77] have conclusively demonstrated that the (1×2) structure on Pd{110} is virtually identical to the clean surface missing row structures, again involving multilayer effects.

Two mechanisms have been suggested for these alkali−metal-induced reconstructions. The first model stresses the importance of long-range effects and was proposed by Ho and co-workers as an extension of their work on clean surface reconstructions.[71,80] It again implies that the reconstruction is induced by the increased delocalization of the s electron density possible at the reconstructed surface. A second model has also been proposed which stresses the importance of short range effects.[64,81] Within this model, the reconstruction is driven by the higher adsorption energy of an alkali metal atom on the reconstructed surface. This model has the advantage of explaining the coverage dependence of the reconstruction. At low coverages (1×2) and (1×3) structures are stabilized by the increased heat of adsorption; the (1×3) structure has deeper channels created by the removal of three close packed rows of the substrate. The structure is highly corrugated and has even been observed on the clean Pt{110} surface.[68,69] On the reconstructed surface, the large alkali metal atoms have a higher number of nearest neighbors and hence a higher adsorption energy. This increase in adsorption energy is enough to stabilise these structures with respect to the (1×1) structure. At higher coverages, the increase in adsorbate−adsorbate repulsion causes the adsorption energy to fall, and the surface reverts to an alkali overlayer on an unreconstructed substrate. It is important to realize that both of these effects operate simultaneously and indeed are different manifestations of the same process. This should be born in mind when considering all models of surface reconstruction; a combination of long-range and short-range effects will play a role in determining the driving force behind the observed effects.

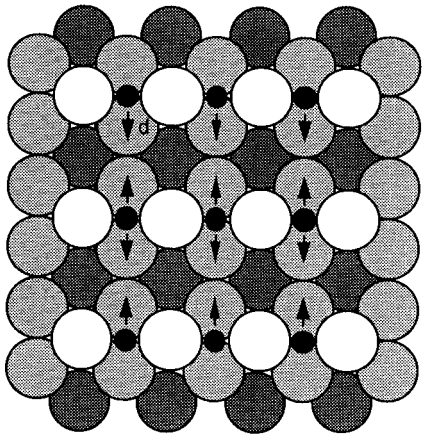

Figure 7. The Cu{110}-(2×1)-O structure, with Cu−O−Cu chains running across the surface, and missing rows of Cu atoms perpendicular to the close packed rows.[92] The large circles are the Cu atoms, with successively deeper layers being represented by darker shading. The small black circles are the oxygen atoms. There is also a small pairing displacement in the second layer of $d = 0.03$ Å.

It is important to note that the adsorbate-induced missing row reconstruction is not a universally observed phenomenon on fcc {110} surfaces. Adsorption of atomic oxygen onto Ni and Cu {110} surfaces gives rise to a (2 ×1) added row reconstruction.[82−95] The removal of alternate Cu atoms along [1$\bar{1}$0] produces missing rows running in the [001] direction, i.e. perpendicular to the close-packed rows and to the missing rows discussed previously, and the adsorption of oxygen atoms in long bridge sites leads to a structure made up of added Cu−O chains along [001].[84−93] A quantitative LEED study on the O−Cu system shows that multilayer relaxations are again important[92] (Figure 7). A similar structure has been found for the O−Ni system.[94,95]

This structure may appear surprising since it involves an increase in the number of broken nearest neighbor bonds and places oxygen atoms in apparently unfavorable long bridge positions. However the driving force behind its formation is the increase in the copper-to-oxygen bond strength that it provides. The low coordination of the Cu atoms in the Cu−O chains causes the filled d band to shift upward

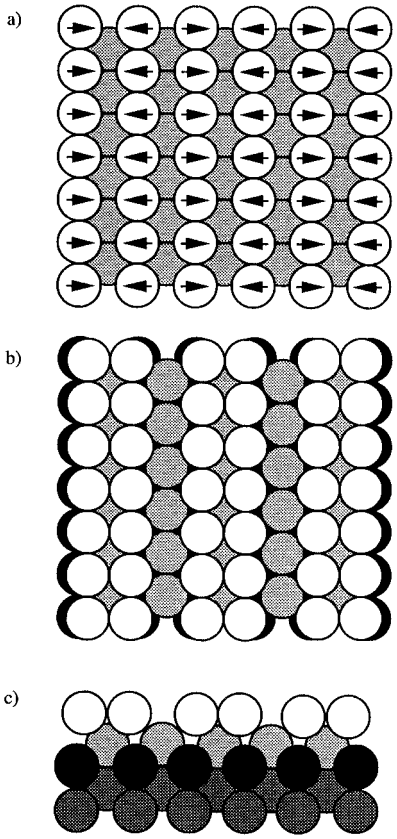

Figure 8. The hydrogen induced paired row reconstruction of Ni{110}.[78] Part a shows the direction of the pairing displacements of the top layer atoms; b shows a plan view of the reconstructed surface, while c shows a cross sectional view. Hydrogen atoms have been omitted for clarity.

toward the Fermi level, causing the antibonding states formed in the interaction with the adsorbed O 2p states, to shift above the Fermi level. This lowering of the occupancy of the antibonding eigenstates gives rise to an increase in the O−Cu bonding.[93]

The reconstructions discussed above are driven by the increase in the adsorbate−substrate bond strength on the reconstructed surface and the change in the local valence electron density at the surface metal atoms caused by bonding to the adatoms.

LEED I(V) analyses[96,97] have shown that the adsorption of atomic hydrogen on Ni and Pd{110} produces another form of reconstruction. At low temperatures (<200 K) coverages in excess of 1 ML induce a paired row reconstruction of the substrate (Figure 8), in which lateral displacements of the top layer atoms by 0.3 ± 0.05 and 0.2 ± 0.05 Å are observed for Ni{110} and Pd{110}, respectively. Although the individual chemisorption energy is lower on the reconstructed surface, the reconstruction creates more adsorption sites, allowing the total adsorption energy to increase, which drives the formation of the metastable (1×2) row paired structure. The paired row reconstruction involves only small atomic displacements so that the activation energy for the process is low and it occurs even at low temperatures. It is therefore surprising to note that STM studies[98,99] of the thermodynamically favored streaked (1×2) phase have suggested that large-scale mass transport *is* involved in the formation of this phase. The reconstruction is observed to

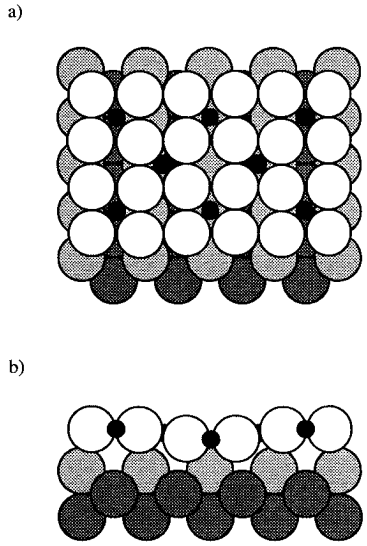

Figure 9. The Cu{110}-(2×3)-N structure.[105] The small dark circles represent the N atoms, the white circles represent the pseudo-{100} layer, and the shaded circles represent the underlying {110} substrate. Part a shows a plan view of the surface, while b displays a cross sectional view through the surface. The outermost, {100}-like, layer is buckled by 0.52 Å by the registry mismatch with the second layer.

be a combined missing row and added row structure. The local character of the reconstruction means that isolated ⟨110⟩ rows of Ni atoms are pulled out of the surface, creating {111} microfacets. EELS,[100] embedded atom method calculations,[101] and time-of-flight scattering and recoiling spectroscopy (TOF-SARS)[102] measurements all suggest that the hydrogen atoms occupy 3-fold sites on the inclined {111} microfacets of the missing and added rows.

Atomic nitrogen adsorption on Cu{110} gives rise to a (2×3) LEED pattern. This structure has been analyzed by a variety of techniques[103−105] and has been shown to consist of a pseudo Cu{100}-c(2×2) overlayer (Figure 9). The overlayer is corrugated by 0.52 Å, with the N atoms virtually coplanar with the first layer Cu atoms. Three of the four nitrogen atoms within the unit cell are 5-fold coordinated (being bonded to a second layer Cu), while the final N atom is 4-fold coordinated. The driving force behind this reconstruction is thought to be the large energy gain for adatoms occupying high coordination sites. The increase in adsorption energy associated with the creation of such a site is again sufficient to overcome the energy lost in reconstructing the clean surface. However, a detailed mechanism for this reconstruction requires further theoretical work.

The last three examples serve to illustrate the complexities involved in adsorbate systems. Although virtually all fcc {110} surfaces reconstruct to the (1×2) missing row structure under certain specific conditions, this is not a universally observed rule. Some systems undergo much more complex reconstructions. The governing principle in these systems is the balance between the increase in adsorption energy of the adsorbate on the reconstructed surface and the corresponding loss of energy created by the surface assuming a nonideal configuration. This energy balance is extremely delicate, giving rise to the wide variety of unusual surface structures observed.

2. Atomic Adsorbates on Other Metal Surfaces

The affinity of N for high coordination sites mentioned above, which drives the (2×3)-Cu{110} reconstruction, is a widely observed phenomenon. On most {100} surfaces, atomic adsorbates occupy 4-fold hollow sites, usually inducing some form of relaxation and buckling; an example is Ni{100}-p(2×2)-O (Figure 10).[106] However, O on Cu{100} gives rise to a structure more similar to the Cu{110}-(2x1)-O structure.[84−93] Again, the O atoms induce a missing row-type reconstruction, with every third row in the ⟨010⟩ direction missing. As in the case of Cu{110}, the oxygen atoms again occupy positions of relatively low coordination giving rise to a $(2\sqrt{2}\times\sqrt{2})$R45° structure shown in Figure 11.[107] The driving force behind this reconstruction is presumably similar to that observed for the Cu{110} surface, although confirmation of this must await further theoretical investigation.

Although atomic adsorbates will usually occupy 4-fold hollow sites on {100} surfaces, they may also induce local reconstructions. On the basis of the observed symmetry of the LEED pattern produced by the Ni{100}-(2×2)-C system, Onuferko et al. proposed a so called "clock reconstruction" model

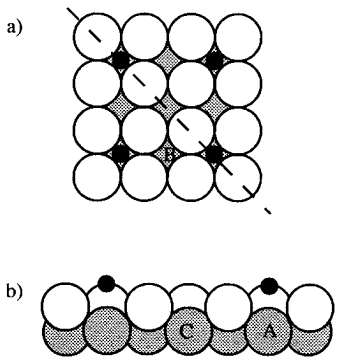

Figure 10. The Ni{100}-p(2×2)-O structure.[106] Part a shows a plan view and b a cross-sectional view. The small dark circles are the O atoms, the larger white circles are the first layer Ni, and the shaded circles are second layer Ni atoms. The Ni atom labeled "C" is displaced upward by 0.055 Å while atom "A" (directly below the O atom) is displaced downward by 0.045 Å. The downward displacement of atom "B", given as 0.005 Å, is beyond the accuracy of the technique. This produces an overall buckling of the second layer by about 0.1 Å.

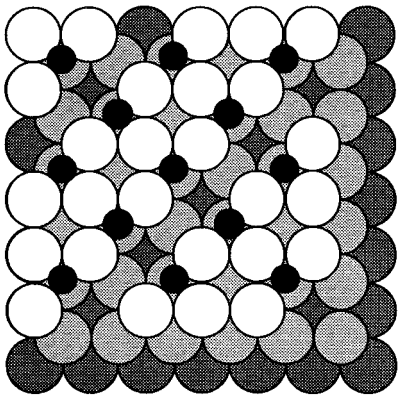

Figure 11. A plan view of the Cu{100}-$(2\sqrt{2}\times\sqrt{2})$R45°-O structure.[107] The local bonding geometry of the O atoms on the step edge is similar to that found in the Cu{110}-(2×1)-O structure (Figure 7).

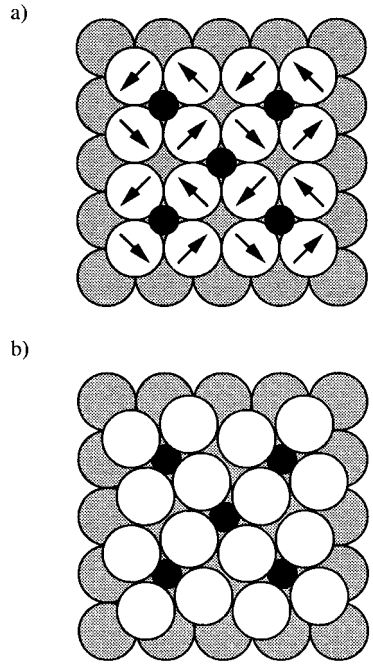

Figure 12. The Ni{100}-(2×2)-C structure—the clock reconstruction. In part a the displacement tendencies of surface atoms away from the ideal 4-fold fcc {100} positions are indicated. Part b displays the resulting structure.[112] The small dark circles are the C atoms while the larger circles are the Ni atoms of the first and second layers.

(Figure 12).[108] In this model, the C atoms are again adsorbed in 4-fold hollow sites, but induce a displacement of the surrounding Ni atoms. These atoms move away from the adsorption site, and rotate about it, opening up the site without significantly altering the Ni−Ni spacing in the top layer (increased by just 4%). Detailed analysis of this system[109−113] supports this model and shows that the C atom is nearly coplanar with the surrounding Ni atoms. The distance between the C and the second layer Ni atom is 1.99 Å, close to the in-plane value of 1.82 Å.[112] Hence, the C atoms are nearly 5-fold coordinated, and it is this trend to adopt or create the highest coordination site which again drives the reconstruction. This mechanism is supported by effective medium calculations, which suggest that the optimum density at a C atom is very high.[114] A similar reconstruction is responsible for the Ni{100}-(2×2)-N structure.[111,115,116]

However, as shown in Figure 10, O does not induce a clocklike reconstruction. Instead, the O atom occupies a 4-fold site, with the second layer Ni atom directly below the adsorption site displaced downward away from the adsorbate, suggesting an antibonding interaction.[106] Wenzel et al.[116] suggest that the different occupancy of the 2p orbitals is responsible for the different behavior exhibited by C, N, and O. The filled $2p_z$ orbital of O does not contribute to the bonding with the surface, whereas for C and N this orbital has a bonding interaction with the second layer Ni atom. This explanation has been supported by the theoretical work of Reindl et al.[117] Consequently, although the vast majority of atomic adsorbates on {100}-type surfaces occupy 4-fold hollow sites, the exact details of the adsorption geometry may be complicated, with some adsorbates managing to induce reconstructions producing pseudo 5-fold coordinated sites on the surface.

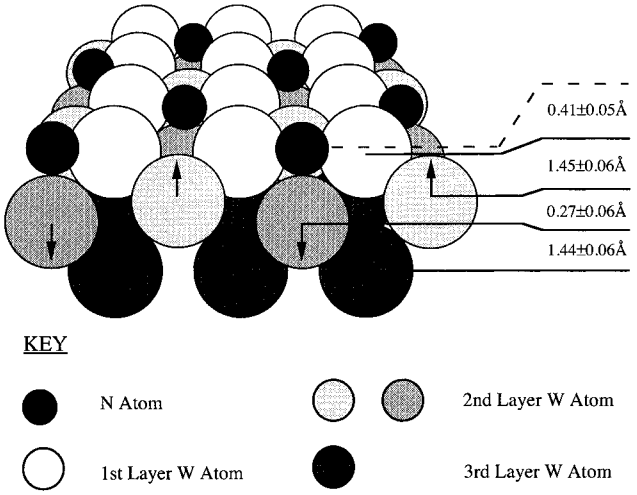

Figure 13. A perspective view of W{100}-c(2×2)-N, with a coplanar top W layer and a buckled second W layer.[120]

The {100} surface of a bcc metal, such as W, has a lower atomic density compared with the fcc surface, and is well known to be unstable with respect to displacive reconstructions, such as the low-temperature zigzag structure of the clean surface (section II.B). Low coverages of atomic hydrogen lead to a change in the nature of the lateral displacements. King and Thomas[118] first suggested that alternate pairs of W atoms are shifted toward each other along ⟨100⟩ producing W dimers, which form a favorable close-bridge H adsorption site. The dimer model has been supported by a recent LEED investigation,[35] which identified the lateral shift to be 0.235 ± 0.045 Å, comparable in magnitude to that observed for the clean surface zigzag reconstruction. In the case of atomic N adsorption, the more open nature of the W{100} surface allows the the adsorbate to adopt pseudo 5-fold coordination in a simple c(2×2) overlayer structure first proposed by Griffiths et al.[119] In a reanalysis, using tensor LEED, Bessent et al.[120] found the N adatom to be 2.13 ± 0.05 Å above the second layer W atom, and 2.27 ± 0.05 Å from the surface layer atoms, of the hollow site, confirming the pseudo-5-fold coordination of the adsorption site. The structure is shown in Figure 13. This study also identified a large buckling of the second substrate layer, reflecting the change in local valence electron density that a N adatom brings to a surface site. At coverages between 0.3 and 0.4 ML the fractional order spots are observed to split into quartets, which have been assigned[121] to the formation of a contracted domain structure. The atoms forming the 4-fold site are thought to be uniformly displaced toward the N atom producing islands of more densely packed surface W atoms, on which the N atoms are closer to true 5-fold coordination. This structure, identified in 1981, is remarkably similar to the (2× 3) Cu{110} reconstruction described above and shown in Figure 9.

Indeed, this drive to occupy high coordination sites is so strong that it may drive reconstructions of fcc {111} surfaces. Just as N produces a pseudo {100} overlayer on the Cu{110} surface, S and C on Ni{111} also induce a pseudo {100}-(2×2) overlayer structure, illustrated in Figure 14.[122−128] The majority of quantitative studies performed to date have

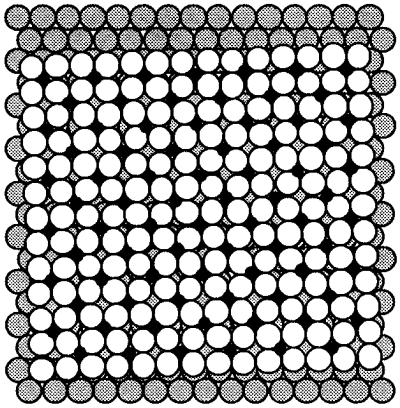

Figure 14. Plan view of the proposed model for sulfur or carbon on Ni{111}. A square fcc {100}-like overlayer is formed sitting on top of an fcc {111} substrate, and rotated with respect to it.[128] Small filled circles, S or C adatoms; unfilled circles, top layer Ni atoms; shaded circles, second layer Ni atoms.

concentrated on the (5√3×2) 0.4 ML S phase. SEXAFS measurements give coordination numbers consistent with 4-fold adsorption sites,[122,123] while a combined STM and X-ray diffraction study suggested that the pseudo {100} layer is further reconstructed into a clock-like pattern.[124] It has also been suggested that fluctuations in the Ni−Ni spacings may occur.[125,126] Recent HREELS and SXPS data[127] supports both these models, suggesting that the overlayer is indeed a modified form of a {100}-like layer. The c(5√3×9)rect structures produced by the adsorption of C and N on Ni{111} appears to be a similar structure. On the basis of LEED I(V) fingerprinting, in which similarities in the I(V) curves from different structures are taken to suggest similar local geometries, Gardin et al.[128] have suggested that the local environment of the C atoms must be very similar to that found for the Ni{100}-(2×2)-C system—the clock reconstruction. This example serves to illustrate the multidisciplinary nature of surface science, with a wide variety of techniques being needed to make sense of complex surface problems.

In some respects this reconstruction is the converse of the Pt{100}-hex reconstruction. In that example, a hexagonal layer is formed on top of a square lattice, whereas here, a square lattice is formed of top of a hexagonal layer. However, when the Pt{100}-hex phase is exposed to most adsorbates the hexagonal top layer reverts to a square layer, lifting the reconstruction. This hexagon to square transition is presumably similar to the process occurring on the Ni{111} surface where again there is a hexagon to square transition in the presence of an adsorbate. The adsorbate increases the local charge on a metal atom, hence in both cases the metal surface is induced to move to a lower atomic density structure restoring the local valence electron density at the surface atoms to the optimum value.

3. Summary of Atomic Adsorbates

The added complexity produced by the introduction of an adsorbate onto the surface has been demonstrated. A few general observations can be made. Fcc {110} surfaces are generally unstable to reconstruction, with adsorbates, but the exact form of the

reconstruction is difficult to predict. A number of adsorbates produce missing row reconstructions, but Cu{110} seems to undergo a wide variety of different reconstructions. These could also occur on other {110} surfaces.

In general, atomic adsorbates tend to favor high coordination adsorption sites which on fcc {100}-type surfaces implies 4-fold hollow sites. Indeed, some adsorbates induce reconstruction of the {100} surface to produce 5-fold coordinated sites, by a clock rotation of top layer metal atoms. This is also observed on some fcc {111} surfaces, where atomic adsorbates may induce reconstructions resulting in 4-fold or even 5-fold sites.

The exact form of the surface geometry is produced by a balance between the energy gained by the surface adopting a less than ideal configuration and the increase in adsorption energy of the adsorbate. This may be a very fine balance, and gives rise to a wide variety of unusual structures.

B. Molecular Adsorbates

The complication added to the structural analysis of atomic adsorbate systems, mentioned previously, is increased in the case of molecular adsorbates. This is reflected by the uncertainty that surrounds the earliest structural determinations of molecular adsorbate induced reconstructions. However, in the last five years much progress has been made, and structural analyses of simple molecular adsorbate systems can now be approached with the same degree of confidence as the atomic adsorbate systems reviewed above. Since one of the aims of surface science is to understand adsorbate−substrate interactions relevant to surface catalyzed reactions, the goal for surface crystallography has to be to extend these studies to larger molecular adsorbates.

The strong influence that molecular adsorbates can exert on surface structure is demonstrated by the observed lifting of the Pt{100}-hex reconstruction by a number of molecules.[129] For the case of CO, the dynamics of the reconstruction to a (1×1) surface have been shown to follow a strongly nonlinear power law,[42] which plays a critical role in the oscillatory nature of the oxidation of CO on Pt{100}.[43−45] Here, adsorption heat measurements demonstrate that the heat is considerably higher—215 kJ mol^{-1}—on the (1×1) surface than on the hex surface without reconstruction, on which it is only 105 kJ mol^{-1}.[56] This difference in adsorption heat is clearly the driving force for the lifting of the hex reconstruction.

As has so often been the case in surface science[130] it was carbon monoxide which provided the starting point for studies of molecular induced reconstruction of initially unreconstructed surfaces. The first conclusive report of a substantial molecular induced reconstruction was provided by Raval et al.[131] on the basis of RAIRS measurements of CO adsorbed on Pd{110}. The results provided further evidence of the tendency of fcc {110} surfaces to reconstruct, as previously discussed in sections II.D and III.A.1. Three adsorption phases, identified as disordered (1×1), (4×2) and (2×1)p1g1, are formed as the CO coverage is increased. The high temperature (>250 K) required for the (4×2) phase to develop implies the existence of a significant activation barrier, suggestive of substantial surface reconstruction. For comparison, temperatures in excess of 280 K are required for the diffusion of Pt atoms necessary to develop the missing row reconstruction of Pt{110}.[132,133] On the basis of a LEED I(V) fingerprinting analysis[134] the underlying Pd substrate was identified as showing the missing row reconstruction discussed in sections II.D and III.A.1. The IR stretching frequency of CO suggests adsorption at a short bridge site, and the driving mechanism for the reconstruction was proposed to be the higher heat of adsorption of CO on the reconstructed surface[131,134] (Figure 15). The missing row reconstruction allows more molecules to occupy the favored 2-fold symmetric short-bridge sites on the {111}-faceted slopes, that have been described previously, while the contrapositioned geometry of these slopes allows the CO charge clouds to be directed away from each other, reducing intermolecular Pauli repulsion. At coverages above 0.75 ML it is not possible to maintain the favored 2-fold occupancy and avoid unfavorable CO−CO interactions. For this reason the reconstruction is lifted, with alternate CO molecules being tilted in opposite directions, while still occupying the favored 2-fold sites, on the (1×1) substrate, giving rise to a (2×1)p1g1 phase. The differential heat of CO adsorption falls substantially as this occurs.[131]

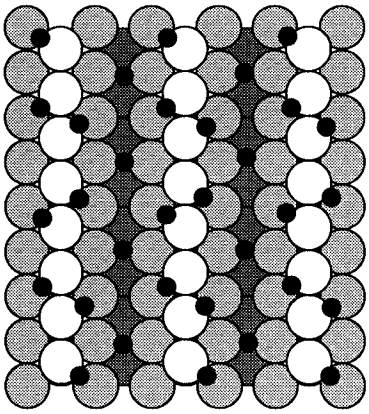

Figure 15. Plan view of the proposed model for the Pd{110}-(4×2)-CO phase. The surface exists in a reconstructed missing row structure, with CO molecules (shown as smaller circles) occupying 2-fold symmetric, short-bridged sites on the, contrapositioned, {111} faceted slopes.[131]

Despite the comparative simplicity of CO as a molecular adsorbate there has been substantial debate concerning the structure of this system.[135] In a tensor LEED study of the high coverage (2×1)p1g1 phase[136] the CO molecules were reported to be adsorbed in atop sites, and to be tilted by 11 ± 4° with respect to the surface normal, in contrast with the assignment from the RAIRS study by Raval et al.[131] and LEED measurements for the Ni{110}-(2×1)-CO surface phase,[137] which both favored 2-fold bridge site occupancy. However, recent local density approximation total energy calculations[138] and photoelectron diffraction data[139] both show a strong preference for the 2-fold site, challenging the findings of the tensor LEED study and supporting the original RAIRS assignment.

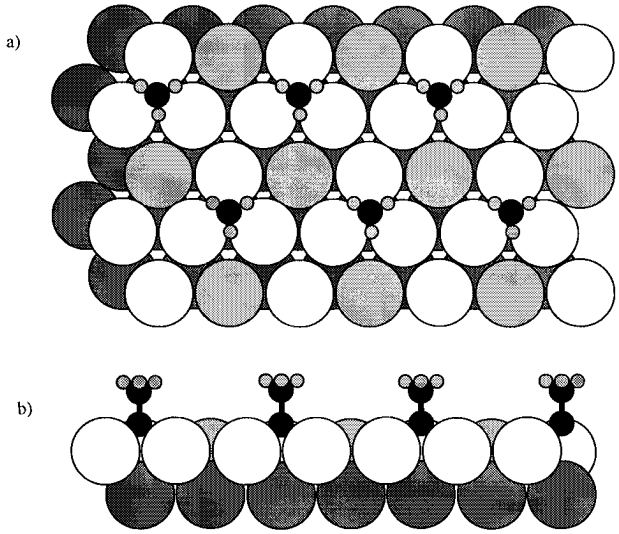

Figure 16. The p(2 × 2) structure of ethylidyne (CCH_3) on Rh{111},[140] shown in (a) plan view, and (b) in cross sectional view. The white atoms relax away from the substrate by 0.12 ± 0.04 Å, the lightly shaded atoms remain at the clean surface positions, and the darker shaded atoms represent the second Rh layer.

This example illustrates that even with a simple molecule, such as CO, the structural analysis of molecular adsorbate systems is far from straightforward. It also demonstrates that molecules, as well as atoms, can induce large-scale reconstructions of the substrate.

Like the atomic adsorbates discussed in section III.A.2 molecules have also been found to induce displacive reconstructions. In a reanalysis of ethylidyne (CCH_3) adsorbed on Rh{111}, by tensor LEED, Wander et al. found the first evidence of such a molecule-induced reconstruction.[140] The ethylidyne molecule is found to adsorb upright in hcp 3-fold hollow sites. The three neighboring Rh atoms are displaced radially outward from the site by 0.05 ± 0.05 Å and lifted out from the surface by 0.12 ± 0.04 Å. The displacement of the Rh atom below the ethylidyne in the second layer is beyond the accuracy of the technique, being reported as an outward lift of 0.01 ± 0.05 Å (Figure 16). Substrate atoms local to the adsorbate are returned to a bulk-like coordination, and consequently relax to bulk-like positions to reduce the local charge density back to the optimal value. The fourth Rh atom of the top layer, which is not bonded to the ethylidyne, remains at its clean surface position, leading to a buckling of the outermost surface layer.

One of the current aims of surface crystallography is to obtain reliable structural information for larger, catalytically relevant, molecules and molecular fragments. One of the problems with such adsorbate systems is that they frequently do not form ordered overlayers, whereas conventional LEED analysis is dependent on long-range order. One approach to solving this problem has come in the form of the development of diffuse LEED.[141,142] One of the first applications of this technique was a study of the adsorption of benzene on Pt{111} by Wander et al.[143] In this study benzene was found to adsorb at a 2-fold bridge site and shows a strong boatlike distortion

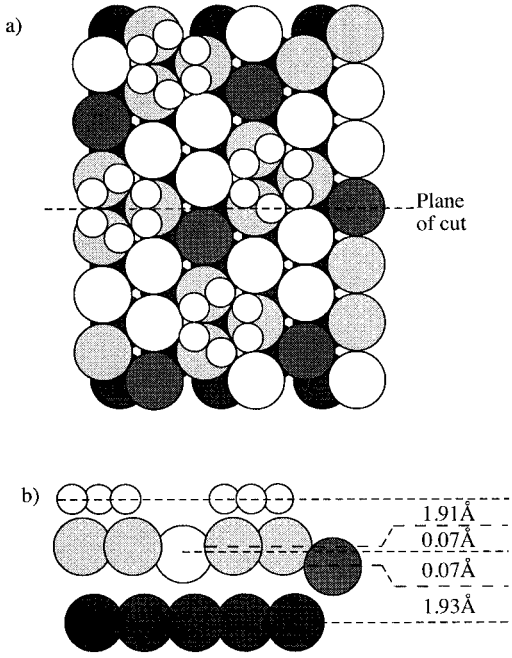

Figure 17. The structure obtained for Ni{111}($\sqrt{(7)}\times\sqrt{(7)}$)R19°-$C_6H_6$, in plan and cross section.[151]

from planarity, with bond lengths of 1.63 ± 0.05 Å and 1.45 ± 0.10 Å. Comparing these values with the C−C single bond length of ~1.54 Å indicates that this represents a substantial distortion of the benzene molecule. The values should also be compared with the gas-phase bond length of 1.397 Å and the value determined by NEXAFS for benzene on Pt{111} of 1.40 ± 0.02 Å.[144] LEED studies of disordered overlayers now generally employ the more reliable diffuse LEED I(V) technique.[145−148] While such substantial distortion of benzene has been reported for coadsorption with CO on Rh{111}[149] it contrasts with the findings of recent LEED studies of pure benzene on Ru{001}[150] and Ni{111}.[151] On Ru{001} benzene adsorbs in a hcp 3-fold hollow site, with only a small crown-like distortion of the ring. Surprisingly, the substrate shows a large *contraction* of the first interlayer spacing, attributed to adsorption of a π-donor. On Ni{111}, the benzene ring shows a small expansion, but retains its planar character, and the first layer of the substrate is strongly buckled due to changes in the local valence electron density. The full structure is shown in Figure 17.

Another example of a catalytically important adsorbate is formate (HCOO), which does not form ordered overlayers on Cu{110} and Cu{100}, systems of relevance to methanol synthesis. Photoelectron diffraction studies[152,153] have shown that the formate molecule adsorbs in a short bridge site, with the oxygen atoms close to atop positions. LCAO-LDF calculations[153] indicated that the short-bridge site was 20 kcal mol^{-1} more stable than the cross-bridge site (Figure 18), in agreement with an earlier calculation by Wander and Holland,[154] and provided a trial geometry for the photoelectron diffraction calculation. The LDF calculation suggests that the short-bridge site is more favorable as it facilitates strong σ-bonding, whereas the cross-bridge site is π-bound. This study indicates the increasingly important role that total energy calculations will play in the determina-

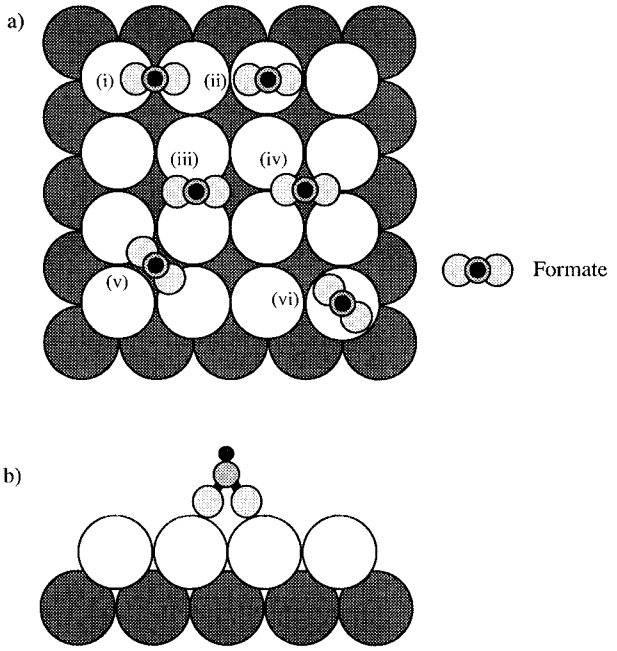

Figure 18. Part a shows the proposed adsorption sites for formate on Cu{100}.[153] LCAO-LDF calculations[153] indicate that the short bridge site (i) is the most stable. Photoelectron diffraction studies[152,153] also identify this as the likely adsorption site, which is shown in cross section in b.

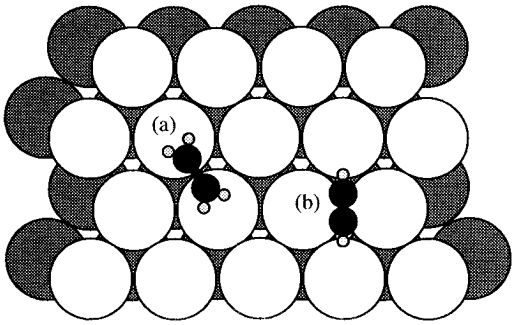

Figure 19. The adsorption sites of (a) ethylene and (b) acetylene on Ni{111}, as determined by photoelectron diffraction, are shown.[155−157]

tion and rationalization of molecular adsorbate structures.

It has previously been mentioned that one of the aims of surface science is to try to understand surface catalysed reactions. An example where local structural information goes some way to achieving this aim is the dehydrogenation of ethylene to acetylene on Ni{111}. Using photoelectron diffraction Bao et al. were able to determine the geometry of ethylene and acetylene adsorbed on Ni{111}.[155−157] In both cases the molecule is adsorbed parallel to the surface, ethylene occupying an aligned bridge site with the carbon atoms approximately above surface nickel atoms, whereas acetylene occupies a cross-bridge site, with the carbon atoms in inequivalent 3-fold hollow sites (Figure 19). This information allowed the authors to propose possible mechanisms by which the dehydrogenation of ethylene may proceed.[156,157] Of course, care must be taken to avoid overinterpretation, as the determination of stable, static structures is only a very indirect guide to structural transitions in dynamic chemical transformations.

A major challenge for surface crystallography is to obtain reliable information of this kind for a wide range of surface catalyzed processes, a goal which necessitates structural studies of a large number of increasingly complex molecular adsorbates.

IV. Summary

In this review we have demonstrated that the rigid lattice picture of surfaces has now been firmly replaced by that of a mobile, plastic surface which responds to changes in surface environment through structural modifications. These structural modifications may take the form of simple interlayer relaxations, displacive intralayer reconstructions, reconstructions involving large scale atom transport, or a combination of all of these effects. On clean surfaces these modifications are associated with the redistribution of surface electronic density, and extend over several layers of the surface region. Atomic adsorbates have been shown to have an affinity for high coordination number adsorption sites, and both long- and short-range effects play important roles in driving the reconstruction of the substrate in these systems, the resulting structure being determined by the balance between the increase in the adsorption energy on the reconstructed surface, and the increase in the surface energy caused by the adoption of a less than ideal configuration. Molecular adsorbates also induce reconstructions, and the challenge to surface crystallography is to extend the structural information that is available for molecular adsorbates to a larger number of catalytically relevant species.

V. Acknowledgments

S. T. acknowledges the EPSRC (U.K.) for a studentship, and Fisons (VG) for additional financial support combined with the Newton Trust.

VI. References

(1) Surface Science. The First Thirty Years *Surf. Sci.* **1994**, 299/300.
(2) *The Chemical Physics of Solid Surfaces*; King, D. A.; Woodruff, D. P., Eds.; Elsevier: Amsterdam, 1980−95; Vols. 1−7.
(3) Noonan, J. R.; Davis, H. L. *Phys. Rev. B* **1984**, *29*, 4349−4355.
(4) Van Hove, M. A.; Tong, S. Y. *Surface Crystallography by LEED*; Springer-Verlag: Berlin, 1979.
(5) Van Hove, M. A.; Moritz, W.; Over, H.; Rous, P. J.; Wander, A.; Barbieri, A.; Materer, N.; Starke, U.; Jentz, D.; Powers, J. M.; Held, G.; Somorjai, G. A. *Surf. Sci.* **1993**, *287*, 428−431.
(6) Woodruff, D. P.; Delchar, T. A. *Modern Techniques of Surface Science*, 2nd ed.; Cambridge University: Cambridge, 1994.
(7) Watson, P. R.; Van Hove, M. A.; Hermann, K. *NIST Surface Structure Data Base - Ver. 1*; National Institute of Standards and Technology: Gaithersburg, 1993.
(8) Pendry J. B. *Low Energy Electron Diffraction*; Academic Press: London, 1974.
(9) Laramore, G. E.; Duke, C. B. *Phys. Rev. B* **1972**, *5*, 267−285.
(10) Jepsen, D. W.; Marcus, P. M.; Jona, F. *Phys. Rev. B* **1972**, *6*, 3684−3690.
(11) Davis, H. L; Noonan, J. R.; Jenkins, L. H. *Surf. Sci.* **1979**, *83*, 559−571.
(12) Adams, D. L.; Nielsen, H. B; Andersen, J. N.; Stensgaard, I.; Feidenhans'l, R.; Sørensen, J. E. *Phys. Rev. Lett.* **1982**, *49*, 669−672.
(13) Davis, H. L.; Noonan, J. R. *Surf. Sci.* **1983**, *126*, 245−252.
(14) Andersen, J. N.; Nielsen, H. B.; Petersen, L.; Adams, D. L. *J. Phys. C* **1984**, *17*, 173−192.
(15) Wander, A.; Barnes, C. J.; Mapledoram, L. D.; King, D. A. *Surf. Sci.* **1993**, *281*, 42−50.
(16) Finis, M. W.; Heine, V. *J. Phys. F* **1974**, *4*, L37−L41.
(17) Landman, U.; Hill, R. N.; Mostoller, M. *Phys. Rev. B* **1980**, *21*, 448−457.

(18) Nørskov, J. K.; Lang, N. D. *Phys. Rev. B* **1980**, *21*, 2131−2136.
(19) Materer, N.; Starke, U.; Barbieri, A.; Döll, R; Heinz, K; Van Hove, M. A.; Somorjai, G. A. *Surf. Sci.* **1995**, *325*, 207−222.
(20) Quinn, J.; Li, Y. S.; Tian, D.; Li, H.; Jona, F.; Marcus, P. M. *Phys. Rev. B* **1990**, *42*, 11348−11351.
(21) Oed, W.; Dötsch, B.; Hammer, L.; Heinz, K.; Müller, K. *Surf. Sci.* **1988**, *207*, 55−65.
(22) Ohtani, H.; Van Hove, M. A.; Somorjai, G. A. *Surf. Sci.* **1987**, *187*, 372−386.
(23) Pettifor, D. G. *J. Phys. F* **1978**, *8*, 219−230.
(24) Methfessel, M.; Hennig, D.; Scheffler, M. *Phys. Rev. B* **1992**, *46*, 4816−4829.
(25) Needs, R. J.; Godfrey, M. J.; Mansfield, M. *Surf. Sci.* **1991**, *242*, 215−221.
(26) Sandy, A. R; Mochrie, S. G. J.; Zehner, D. M.; Grübel, G.; Huang, K. G.; Gibbs, D. *Phys. Rev. Lett.* **1992**, *68*, 2192−2195.
(27) Perdereau, J.; Biberian, J. P.; Rhead, G. E. *J. Phys. F* **1974**, *4*, 798−806.
(28) Feibelman, P. J.; Nelson, J. S.; Kellog, G. L. *Phys. Rev. B* **1994**, *49*, 10548−10556.
(29) Debe, M. K.; King, D. A. *Phys. Rev. Lett.* **1977**, *39*, 708−711.
(30) Walker, J. A.; Debe, M. K.; King, D. A. *Surf. Sci.* **1981**, *104*, 405−418.
(31) Fu, C. L.; Freeman, A. J. *Phys. Rev. B* **1988**, *37*, 2685−2688.
(32) Fasolino, A.; Santoro, G.; Tosatti, E. *Phys. Rev. Lett.* **1980**, *44*, 1684−1687.
(33) Altman, M. S.; Estrup, P. J.; Robinson, I. K. *Phys. Rev. B* **1988**, *38*, 5211−5214.
(34) Landskron, H.; Bickel, N.; Heinz, K.; Schmidtlein, G.; Müller, K. *J. Phys.: Condens. Matter* **1989**, *1*, 1−12.
(35) Schmidt, G.; Zagel, H.; Landskron, H.; Heinz, K.; Müller, K.; Pendry, J. B. *Surf. Sci.* **1992**, *271*, 416−426.
(36) Jupille, J.; King, D. A. In *The Chemical Physics of Solid Surfaces*; King, D. A., Woodruff, D. P., Eds.; Elsevier: Amsterdam, 1994; Vol. 7, pp 35−73.
(37) Hagstrom, S.; Lyon, H. B.; Somorjai, G. A. *Phys. Rev. Lett.* **1965**, *15*, 491−493.
(38) Heilmann, P.; Heinz, K.; Müller, K. *Surf. Sci.* **1979**, *83*, 487−497.
(39) Fedak, D. G.; Gjostein, N. A. *Phys. Rev. Lett.* **1966**, *16*, 171−172.
(40) Fedak, D. G.; Gjostein, N. A. *Surf. Sci.* **1967**, *8*, 77−97.
(41) Grant, J. T. *Surf. Sci.* **1969**, *18*, 228−238.
(42) Hopkinson, A.; Bradley, J. M.; Guo, X.-C.; King, D. A. *Phys. Rev. Lett.* **1993**, *71*, 1597−1600.
(43) Gruyters, M.; King, D. A. *J. Chem. Soc., Faraday Trans. 1*, in press.
(44) Hopkinson, A.; King, D. A. *Chem. Phys.* **1993**, *177*, 433−452.
(45) Gruyters, M.; Ali, T.; King D. A. *Chem. Phys. Lett.* **1995**, *232*, 1−6.
(46) Van Hove, M. A.; Koestner, R. J.; Stair, P. C.; Bibérian, J. P.; Kesmodel, L. L.; Bartos, I.; Somorjai, G. A. *Surf. Sci.* **1981**, *103*, 189−217.
(47) Van Hove, M. A.; Koestner, R. J.; Stair, P. C.; Bibérian, J. P.; Kesmodel, L. L.; Bartos, I.; Somorjai, G. A. *Surf. Sci.* **1981**, *103*, 218−238.
(48) Norton, P. R.; Davies, J. A.; Jackson, D. P.; Matsunami, N. *Surf. Sci.* **1979**, *85*, 269−275.
(49) Lang, E.; Müller, K.; Heinz, K.; Van Hove, M. A.; Koestner, R. J.; Somorjai, G. A. *Surf. Sci.* **1983**, *127*, 347−365.
(50) Guo, X.-C.; Hopkinson, A.; Bradley, J. M.; King, D. A. *Surf. Sci.* **1992**, *278*, 263−269.
(51) Behm, R. J.; Hösler, W; Ritter, E.; Binnig, G. *Phys. Rev. Lett.* **1986**, *56*, 228−231.
(52) Borg, A.; Hilmen, A.-M.; Bergene, E. *Surf. Sci.* **1994**, *306*, 10−20.
(53) Harten, U.; Lahee, A. M.; Toennies, J. P.; Wöll, Ch. *Phys. Rev. Lett.* **1985**, *54*, 2619−2622.
(54) Wöll, Ch.; Chiang, S; Wilson, R. J.; Lippel, P. H. *Phys. Rev. B* **1989**, *39*, 7988−7991.
(55) Fiorentini, V.; Methfessel, M.; Scheffler, M. *Phys. Rev. Lett.* **1993**, *71*, 1051−1054.
(56) Yeo, Y. Y.; Wartnaby, C. E.; King, D. A. *Science* **1995**, *268*, 1731−1732.
(57) Moritz, W.; Wolf, D. *Surf. Sci.* **1979**, *88*, L29−L34.
(58) Adams, D. L.; Nielsen, H. B.; Van Hove, M. A.; Ignatiev, A. *Surf. Sci.* **1981**, 104, 47−62.
(59) Chan, C.-M.; Van Hove, M. A.; Weinberg, W. H.; Williams, E. D. *Solid State Commun.* **1979**, *30*, 47−49.
(60) Koch, R.; Borbonus, M.; Haase, O.; Rieder, K. H. *Appl. Phys. A* **1992**, *55*, 417−429.
(61) Koch, R; Borbonus, M.; Haase, O; Rieder, K. H. *Phys. Rev. Lett.* **1991**, *67*, 3416−3419.
(62) Hayden, B. E.; Prince, K. L.; Davie, P. J.; Paolucci, G; Bradshaw, A. M. *Solid State Commun.* **1983**, *48*, 325−327.
(63) Barnes, C. J.; Ding, M. Q.; Lindroos, M.; Diehl, R. D.; King, D. A. *Surf. Sci.* **1985**, *162*, 59−73.
(64) Behm, R. J.; Flynn, D. K.; Jamison, K. D.; Ertl, G.; Thiel, P. A. *Phys. Rev. B* **1987**, *36*, 9267−9270.
(65) Moritz, W.; Wolf, D. *Surf. Sci.* **1985**, *163*, L655−L665.
(66) Vlieg, E.; Robinson, I. K.; Kern, K. *Surf. Sci.* **1990**, *233*, 248−254.
(67) Sowa, E. C.; Van Hove, M. A.; Adams, D. L. *Surf. Sci.* **1988**, *199*, 174−182.
(68) Fery, P.; Moritz, W.; Wolf, D. *Phys. Rev. B* **1988**, 38, 7275−7286
(69) Binnig, G.; Rohrer, H.; Gerber, Ch.; Weibel, E. *Surf. Sci.* **1983**, *131*, L379−L384.
(70) Gritsch, T.; Coulman, D.; Behm, R. J.; Ertl, G. *Surf. Sci.* **1991**, *257*, 297−306.
(71) Ho, K.-M.; Bohnen, K. P. *Phys. Rev. Lett.* **1987**, *59*, 1833−1836.
(72) Reimer, W.; Penka, V.; Skottke, M.; Behm, R. J.; Ertl, G. *Surf. Sci.* **1987**, *186*, 45−54.
(73) Adams, D. L.; Nielsen, H. B.; Andersen, J. N. *Surf. Sci.* **1983**, *128*, 294−310.
(74) Diehl, R. D.; Lindroos, M.; Kearsley, A.; Barnes, C. J.; King, D. A. *J. Phys. C* **1985**, *18*, 4069−4076.
(75) Skottke, M.; Behm, R. J.; Ertl, G.; Penka, V.; Moritz, W. *J. Chem. Phys.* **1987**, *87*, 6191−6198.
(76) Lindroos, M.; Barnes, C. J.; Valden, M.; King, D. A. *Surf. Sci.* **1989**, *218*, 269-282.
(77) Barnes, C. J.; Lindroos, M.; King, D. A. *Surf. Sci.* **1988**, *201*, 108−128.
(78) Barnes, C. J. In *The Chemical Physics of Solid Surfaces*; King, D. A., Woodruff, D. P., Eds.; Elsevier: Amsterdam, 1994; Vol. 7, pp 501−571.
(79) Marbrow, R. A.; Lambert, R. M. *Surf. Sci.* **1976**, *61*, 329−342.
(80) Fu, C. L.; Ho, K. M. *Phys. Rev. Lett.* **1989**, *63*, 1617−1620.
(81) Jacobsen, K. W.; Nørskov, J. K. *Phys. Rev. Lett.* **1988**, *60*, 2496−2498.
(82) Mac Rae, A. U. *Surf. Sci.* **1964**, *1*, 319−348.
(83) Ertl, G. *Surf. Sci.* **1967**, *6*, 208−232.
(84) Besenbacher, F.; Stensgaard, I. In *The Chemical Physics of Solid Surfaces*; King, D. A.; Woodruff, D. P., Eds.; Elsevier: Amsterdam, 1994; Vol. 7, pp 573−629.
(85) Coulman, D. J.; Wintterlin, J.; Behm, R. J.; Ertl, G. *Phys. Rev. Lett.* **1990**, *64*, 1761−1764.
(86) Jensen, F.; Besenbacher, F.; Laegsgaard, E.; Stensgaard, I. *Phys. Rev. B* **1990**, *41*, 10233−10236.
(87) Kuk, Y.; Chua, F. M.; Silverman, P. J.; Meyer, J. A. *Phys. Rev. B* **1990**, *41*, 12393−12402.
(88) Bronckers, R. P. N; de Wit, A. G. J. *Surf. Sci.* **1981**, *112*, 133−152.
(89) Lapujoulade, J.; Cruër, Y.; Lefort, M.; Lejay, Y; Maurel, E. *Surf. Sci.* **1982**, *118*, 103−120.
(90) Bader, M.; Puschmann, A.; Ocal, C.; Haase, J. *Phys. Rev. Lett.* **1986**, *57*, 3273−3276.
(91) Robinson, A. W.; Somers, J. S.; Ricken, D. E.; Bradshaw, A. M.; Kilcoyne, A. L. D.; Woodruff, D. P. *Surf. Sci.* **1990**, *227*, 237−245.
(92) Parkin, S. R.; Zeng, H. C.; Zhou, M. Y.; Mitchell, K. A. R. *Phys. Rev. B* **1990**, *41*, 5432−5435.
(93) Jacobsen, K. W.; Nørskov, J. K. *Phys. Rev. Lett.* **1990**, *65*, 1788−1791.
(94) Kleinle, G. J.; Wintterlin, J.; Ertl, G.; Behm, R. J.; Jona, F.; Moritz, W. *Surf. Sci.* **1990**, *225*, 171−183.
(95) Eierdal, L.; Besenbacher, F.; Laegsgaard, E.; Stensgaard, I. *Ultramicroscopy* **1992**, *42−44*, 505−510.
(96) Kleinle, G.; Penka, V.; Behm, R. J.; Ertl, G.; Moritz, W. *Phys. Rev. Lett.* **1987**, *58*, 148−151.
(97) Kleinle, G.; Skottke, M.; Penka, V.; Ertl, G.; Behm, R. J.; Moritz, W. *Surf. Sci.* **1987**, *189/190*, 177−184.
(98) Nielsen, L. P.; Besenbacher, F.; Laegsgaard, E.; Stensgaard, I. *Phys. Rev. B* **1991**, *44*, 13156−13159.
(99) Stensgaard, I.; Ruan, L.; Besenbacher, F.; Jensen, F.; Laegsgaard, E. *Surf. Sci.* **1992**, *269/270*, 81−88.
(100) Jo, M.; Onchi, M.; Nishijima, M. *Surf. Sci.* **1985**, *154*, 417−434.
(101) Nordlander, P.; Holloway, S.; Nørskov, J. K. *Surf. Sci.* **1984**, *136*, 59−81.
(102) Bu, H.; Roux, C. D.; Rabalais, J. W. *Surf. Sci.* **1992**, *271*, 68−80.
(103) Ashwin, M. J.; Woodruff, D. P. *Surf. Sci.* **1990**, *237*, 108−115.
(104) Robinson, A. W.; Woodruff, D. P.; Somers, J. S.; Kilcoyne, A. L. D.; Ricken, D. E.; Bradshaw, A. M. *Surf. Sci.* **1990**, *237*, 99−107.
(105) Vu, D. T.; Mitchell, K. A. R. *Phys. Rev. B* **1994**, *49*, 11515−11518.
(106) Oed, W.; Lindner, H.; Starke, U.; Heinz, K.; Müller, K.; Saldin, D. K.; de Andres, P.; Pendry, J. B. *Surf. Sci.* **1989**, *225*, 242−248.
(107) Zeng, H. C.; McFarlane, R. A.; Mitchell, K. A. R. *Surf. Sci.* **1989**, *208*, L7−L14.
(108) Onuferko, J. H.; Woodruff, D. P.; Holland, B. W. *Surf. Sci.* **1979**, *87*, 357−374.
(109) Bader, M.; Ocal, C.; Hillert, B.; Haase, J.; Bradshaw, A. M. *Phys. Rev. B* **1987**, *35*, 5900−5902.
(110) Arvanitis, D.; Baberschke, K.; Wenzel, L. *Phys. Rev. B* **1988**, *37*, 7143−7146.
(111) Kilcoyne, A. L. D.; Woodruff, D. P.; Robinson, A. W.; Lindner, Th.; Somers, J. S.; Bradshaw, A. M. *Surf. Sci.* **1991**, *253*, 107−115.

(112) Gauthier, Y.; Baudoing-Savois, R.; Heinz, K.; Landskron, H. *Surf. Sci.* **1991**, *251/252*, 493−497.
(113) Klink, C.; Olesen, L.; Besenbacher, F.; Stensgaard, I.; Laegsgaard, E.; Lang, . N. D. *Phys. Rev. Lett.* **1993** , *71*, 4350−4353.
(114) Nørskov, J. K. *Rep. Prog Phys.* **1990**, *53*, 1253−1295.
(115) Daum, W.; Lehwald, S.; Ibach, H. *Surf. Sci.* **1986**, *178*, 528−536.
(116) Wenzel, L.; Arvanitis, D.; Daum, W.; Rotermund, H. H.; Stöhr, J.; Baberschke, K.; Ibach, H. *Phys. Rev. B* **1987**, *36*, 7689−7692.
(117) Reindl, S.; Aligia, A. A.; Bennemann, K. H. *Surf. Sci.* **1988**, *206*, 20−28.
(118) King, D. A.; Thomas, G. *Surf. Sci.* **1980**, *92*, 201−236.
(119) Griffiths, K.; King, D. A.; Aers, G. C.; Pendry, J. B. *J. Phys. C* **1982**, *15*, 4921−4931.
(120) Bessent, M. P.; Hu, P.; Wander, A.; King, D. A. *Surf. Sci.* **1995**, *325*, 272−278.
(121) Griffiths, K; Kendon, C.; King, D. A.; Pendry, J. B. *Phys. Rev. Lett.* **1981**, *46*, 1584−1587.
(122) Warburton, D. R.; Wincott, P. L.; Thornton, G.; Quinn, F. M.; Norman, D. *Surf. Sci.* **1989**, *211/212*, 71−81.
(123) Kitajima, Y.; Yokoyama, Y.; Ohta, T.; Funabashi, M.; Kosugi, N.; Kuroda, H. *Surf. Sci.* **1989**, *214*, L261−L269.
(124) Foss, M.; Feidenhans'l, R.; Nielsen, M.; Findeisen, E.; Johnson, R. L.; Buslaps, T.; Stensgaard, I.; Besenbacher, F. *Phys. Rev. B* **1994**, *50*, 8950−8953.
(125) Woodruff, D. P. *Phys. Rev. Lett.* **1994**, 72, 2499.
(126) Ruan, L.; Stensgaard, I.; Besenbacher, F.; Laegsgaard, E. *Phys. Rev. Lett.* **1993**, *71*, 2963−2966.
(127) Mullins, D. R.; Huntley, D. R.; Overbury, S. H. *Surf. Sci.* **1995**, *323*, L287−L292.
(128) Gardin, D. E.; Batteas, J. D.; Van Hove, M. A.; Somorjai, G. A. *Surf. Sci.* **1993**, *296*, 25−35.
(129) Morgan, A. E.; Somorjai, G. A. *Surf. Sci.* **1968**, *12*, 405−425.
(130) Yates, J. T., Jr. *Surf. Sci.* **1994**, *299/300*, 731−741.
(131) Raval, R.; Haq, S.; Harrison, M. A.; Blyholder, G.; King, D. A. *Chem. Phys. Lett.* **1990**, *167*, 391−398.
(132) Hofmann, P.; Bare, S. R.; King, D. A. *Surf. Sci.* **1982**, *117*, 245−256.
(133) Jackman, T. E.; Davies, J. A.; Jackson, D. P.; Unertl, W. N.; Norton, P. R. *Surf. Sci.* **1982**, *120*, 389−412.
(134) Hu, P.; Morales de la Garza, L.; Raval, R.; King, D. A. *Surf. Sci.* **1991**, *249*, 1−7.
(135) Raval, R. *Surf. Sci.* **1995**, *331−333*, 1−10.
(136) Wander, A.; Hu, P.; King, D. A. *Chem. Phys. Lett.* **1993**, *201*, 393−398.
(137) Hannaman, D. J.; Passler, M. A. *Surf. Sci.* **1988**, *203*, 449−462.
(138) Hu, P.; King, D. A.; Crampin, S.; Lee, M.-H.; Payne, M. C. *Chem. Phys. Lett.* **1994**, *230*, 501−506.
(139) Locatelli, A.; Brena, B.;Lizzit, S.; Comelli, G.; Cautero, G.; Paolucci, G.; Rosei, R. *Phys. Rev. Lett.* **1994**, *73*, 90−93.
(140) Wander, A.; Van Hove, M. A.; Somorjai, G. A. *Phys. Rev. Lett.* **1991**, *67*, 626-628.
(141) Pendry, J. B.; Saldin, D. K. *Surf. Sci.* **1983**, *145*, 33−47.
(142) Saldin, D. K.; Pendry, J. B.; Van Hove, M. A.; Somorjai, G. A. *Phys. Rev. B* **1985**, *31*, 1216−1218.
(143) Wander, A.; Held, G.; Hwang, R. Q.; Blackman, G. S.; Xu, M. L.; de Andres, P.; Van Hove, M. A.; Somorjai, G. A. *Surf. Sci.* **1991**, *249*, 21−34.
(144) Horsley, J. A.; Stöhr, J.; Hitchcock, A. P.; Newbury, D. C.; Johnson, A. L.; Sette, F. *J. Chem. Phys.* **1985**, *83*, 6099−6107.
(145) Hu, P.; Barnes, C. J.; King, D. A. *Phys. Rev. B* **1992**, *45*, 13595−13598.
(146) Starke, U.; Heinz, K.; Materer, N.; Wander, A.; Michl, M.; Döll, R.; Van Hove, M. A.; Somorjai, G. A. *J. Vac. Sci. Technol. A* **1992,** *10*, 2521−2528.
(147) Heinz, K.; Starke, U.; Bothe, F. *Surf. Sci.* **1991**, *243*, L70−L73.
(148) Barnes, C. J.; Wander, A.; King, D. A. *Surf. Sci.* **1993**, *281*, 33−41.
(149) Barbieri, A.; Van Hove, M. A.; Somorjai, G. A. *Surf. Sci.* **1994**, *306*, 261−268.
(150) Stellwag, C.; Held, G.; Menzel, D. *Surf. Sci.* **1995**, *325*, L379−L384.
(151) Held, G.; Bessent, M. P.; Titmuss, S.; King, D. A. Submitted for publication.
(152) Woodruff, D. P.; McConville, C. F.; Kilcoyne, A. L. D.; Lindner, Th.; Somers, J.; Surman, M.; Paolucci, G.; Bradshaw, A. M. *Surf. Sci.* **1988**, *201*, 228−244.
(153) Sambi, M.; Granozzi, G.; Casarin, M.; Rizzi, G. A.; Vittadini, A.; Caputi, L. S.; Chiarello, G. *Surf. Sci.* **1994**, *315*, 309−322.
(154) Wander, A.; Holland, B. W. *Surf. Sci.* **1988**, *203*, L637−L641.
(155) Bao, S.; Hofmann, Ph.; Schindler, K.-M.; Fritzsche, V.; Bradshaw, A. M.; Woodruff, D. P.; Casado, C.; Asensio, M. C. *Surf. Sci.* **1994**, *307−309*, 722−727.
(156) Bao, S.; Hofmann, Ph.; Schindler, K.-M.; Fritzsche, V.; Bradshaw, A. M.; Woodruff, D. P.; Casado, C.; Asensio, M. C. *Surf. Sci.* **1995**, *323*, 19−29.
(157) Bao, S.; Hofmann, Ph.; Schindler, K.-M.; Fritzsche, V.; Bradshaw, A. M.; Woodruff, D. P.; Casado, C.; Asensio, M. C. *J. Phys.: Condens. Matter* **1994**, *6*, L93−L98.

CR950214C